

HIGH-ENERGY GAMMA-RAY BEAMS FROM COMPTON-BACKSCATTERED LASER LIGHT\*

A.M. Sendorfi, M.J. Levine, C.E. Thorn, G. Giordano\* and G. Matone\*  
 Physics Department, Brookhaven National Laboratory  
 Upton, New York 11973

Summary

Collisions of light photons with relativistic electrons have previously been used to produce polarized  $\gamma$ -ray beams with modest ( $\sim 10\%$ ) resolution, but relatively low intensity. In contrast, the LEGS<sup>1</sup> project (Laser-Electron Gamma Source) at Brookhaven will produce a very high flux ( $> 2 \times 10^7 \text{ s}^{-1}$ ) of background-free polarized  $\gamma$  rays whose energy will be determined to a high accuracy ( $\Delta E \approx 2.3 \text{ MeV}$ ). Initially, 300(420)-MeV  $\gamma$  rays will be produced by backscattering UV light from the new 2.5(3.0)-GeV X-ray storage ring of the National Synchrotron Light Source (NSLS). The LEGS facility will operate as one of many passive users of the NSLS. In a later stage of the project, a Free Electron Laser is expected to extend the  $\gamma$ -ray energy up to 700 MeV.

Introduction

Since 1963 backward Compton scattering of laser light from a high-energy electron beam has been a promising method of producing useful yields of quasi-monochromatic polarized photons.<sup>2)</sup> The scattering process is shown schematically in Fig. 1 (with angles

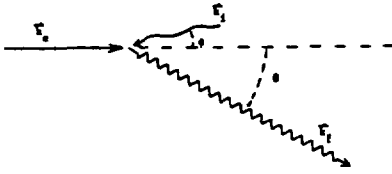


Fig. 1 Schematic of laser + electron backscattering.

greatly magnified). The laser photon and the electron approach each other at some relative angle  $\phi$ . After backscattering, the  $\gamma$  ray emerges at a small angle  $\theta$  relative to the electron beam direction. Because of sequential angular compressions from the Lorentz transformations, the final  $\gamma$ -ray energy is almost completely unaffected by the initial finite divergences that contribute to  $\phi$ . To an excellent approximation, the  $\gamma$ -ray energy is given by

$$E = \frac{4\gamma^2 \epsilon_L}{1 + \frac{4\gamma \epsilon_L}{mc^2} + \theta^2 \gamma^2} \quad (1)$$

where  $\epsilon_L$  is the energy of a laser photon and  $\gamma mc^2$  is the electron beam energy. The highest energy  $\gamma$  rays are traveling at  $\theta \approx 0^\circ$  relative to the electron direction. The resolution of this  $\gamma$  ray beam could thus be determined by collimation. However, in any practical situation the scattering angle cannot be defined to better than the electron beam divergence ( $\theta_e$ ), and thus for electrons with energy resolution  $\Delta E_e$ , the resolution attainable with a collimator (whose half-angle is  $\theta_c$ ) is

$$\frac{\Delta E_\gamma}{E_\gamma} \approx \left[ \left( \frac{2\Delta E_e}{E_e} \right)^2 + (\gamma \Delta \theta)^4 \right]^{1/2}, \quad (2.1)$$

where

\* Work supported by DOE contract DE-AC02-76CH00016.  
 + Address: INFN-Laboratori Nazionali di Frascati, Italy.

$$\Delta \theta = \left( \theta_e^2 + \theta_c^2 \right)^{1/2}. \quad (2.2)$$

The cross sections for  $\gamma$ -ray production by laser backscattering are compressed into a narrow region about  $\theta_{lab} \approx 0^\circ$  by the Lorentz transformations. The extent of this compression increases roughly as the square of the electron energy. This is evident in Fig. 2 where the dependence of the lab cross section upon angle is plotted for 3.0 eV laser light incident upon 0.7 GeV electrons (dashed curve) and upon 2.5 GeV electrons (solid curve). The dependence of the backscattered  $\gamma$ -ray energy, determined from Eq. (1), is

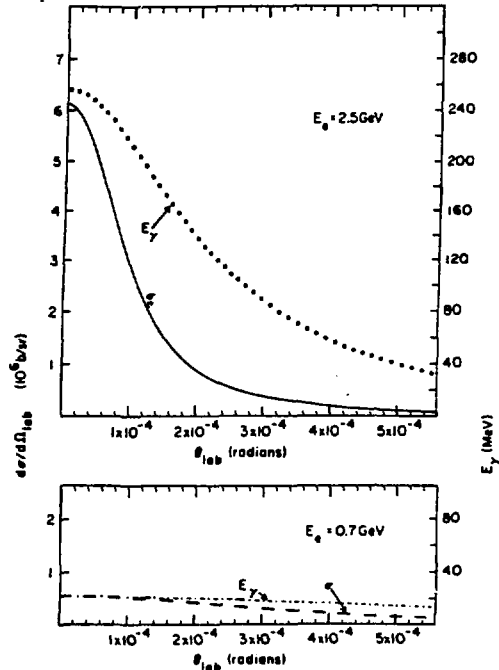


Fig. 2 Cross-section (LH) and energy (RH) variations.

also shown with its scale on the right (dot-dashed and open-circled curves, respectively). As can be seen from this energy variation with angle, collimation of the  $\gamma$  rays can produce a quasi-monoenergetic beam, but the requirements of a small electron divergence  $\theta_e$  become severe at high energies.

The total  $\gamma$ -ray spectrum produced by 3.0 eV laser light incident upon 2.5 GeV electrons is plotted in Fig. 3. (This is effectively the solid curve of Fig. 2, per unit solid angle, plotted against the open-circled curve of Fig. 2). All of the  $\gamma$  rays capable of producing nuclear reactions are contained within  $10^{-3}$  radians of the electron beam direction.

Previous Successes

The first experiment to actually use laser-backscattered photons as a beam in a physics measurement was conducted at SLAC.<sup>3)</sup> Here, 1.78 eV light from a Ruby laser collided with 20 GeV electrons

NOTICE  
 PORTIONS OF THIS REPORT ARE ILLISIBLE.

It has been reproduced from the best available copy to permit the broadest possible dissemination.

DISTRIBUTION OF THIS DOCUMENT IS UNLIMITED

EMB

MASTER

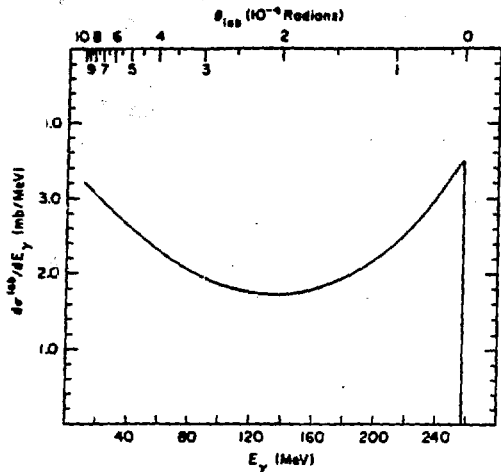


Fig. 3  $\gamma$ -ray spectrum from 3 eV light on 2.5 GeV  $e^-$ .

from the SLAC linac to produce up to 5 GeV  $\gamma$  rays, and a massive hydrogen bubble chamber, acting as both target and detector, compensated for the very low fluxes ( $\sim 500 \text{ s}^{-1}$ ) that were produced. The beam entering the bubble chamber was collimated and resolutions of  $\sim 10\%$  were achieved. Following the extension of the linac to 30 GeV, a new series of measurements has begun using a frequency-quadrupoled Yag laser to produce up to 20 GeV photons. These experiments are ongoing.

To achieve flux levels in the  $\gamma$ -ray beam that are useful for nuclear physics research, very high electron currents are required - on the order of one ampere. These currents can only be achieved in storage rings, and a straight electron-laser interaction region, in which the dimensions and angular divergences of the stored beam are small, is required to achieve high luminosity.

The first real  $\gamma$ -ray "beam" for nuclear physics research was developed at the 1.5 GeV ADONE storage ring at Frascati National Laboratories.<sup>4)</sup> The 2.41 eV light from an external Argon-Ion laser, pulsed to provide photon bunches at the same frequency as the storage ring, was arranged in time to collide head-on with an electron bunch in the middle of a straight section. The angular divergence of the ADONE electron beam is about  $1 \times 10^{-4}$  radians, and this defines the minimum collimation angle and resolution (Eq. 2). This facility has delivered up to  $5 \times 10^4 \text{ s}^{-1}$  polarized  $\gamma$  rays, variable in energy up to 80 MeV with about 7% resolution.

A second phase of the Frascati project is currently under development. In the first phase described above, an Argon-Ion laser, was pulsed with an optical cavity dumper to provide external 20 W light pulses, 15 ns in length. A laser can be regarded as being made up of two components: a plasma tube and an optical cavity. The internal laser power, the light intensity outside the plasma tube but inside the optical cavity, is approximately 10 times larger than the available external power output. In the new setup, the optical cavity of the Argon laser has been stretched to 17.5 meters to encompass the straight section and the entrance and exit dipole magnets. The electron beam can now pass through the optical cavity and collide with the internal laser power. The laser must still be pulsed so that the collisions with the

electrons take place only in the straight section and not in regions of quadrupoles or dipoles where the angular divergence is worse and where the beam direction is not aligned with the  $\gamma$ -ray collimator. A new mode-locking technique has been developed and provides 200 W pulses. The factor of 10 increase in peak laser power has increased the flux to about  $5 \times 10^5$   $\gamma$  rays per second up to 80 MeV in energy.

### The LEGS Facility

The X-ray ring at the NSLS will operate at an energy (2.5-3.0 GeV) that is almost a factor of 2 higher than that of ADONE, and this will result in a factor of 4 increase in the backscattering cross section. Furthermore, the X-ray ring electron beam will reach a factor of 5 higher stored current with a cross sectional area in the straight sections which is a factor of 10 smaller than that of ADONE. As a result of all of these enhancement factors, the BNL facility will be able to produce a high intensity beam ( $> 2 \times 10^7$  photons per second) by techniques much simpler than those forced upon the Frascati group.

The determination of the  $\gamma$ -ray beam energy at LEGS will be achieved by tagging, an approach fundamentally different from the method of collimation. For the spectrum of Fig. 3, the cone of Compton scattered electrons is collapsed a factor of 10 smaller than the already narrow  $\gamma$ -ray cone (i.e., their transverse phase space is negligibly different from that of the stored beam.) The storage-ring dipole magnet immediately following the straight interaction section momentum analyzes these scattered electrons. The  $\gamma$ -ray spectrum of Fig. 3 extends down to zero energy, and the corresponding scattered electrons become indistinguishable from the primary beam. However, all of the electrons associated with a high energy portion of the full backscattered spectrum can easily be separated from the primary beam and transported to a focal plane of the dipole magnet. The energy of the  $\gamma$  ray reaching the nuclear target is then defined by the position of its tagging electron on this focal plane. Septum magnets located after the storage-ring dipole improve the effective dynamic range and resolution of this tagging procedure. For the spectrometer described in the next section, the net photon energy resolution will be about 2.3 MeV for all  $\gamma$ -ray energies. The tagging efficiency is 100% within the dynamic range of the spectrometer,  $E_\gamma > 175 \text{ MeV}$ . (If necessary, this limit can be lowered by using a lower electron energy.) The lower energy  $\gamma$  rays, whose corresponding electrons are outside of the dynamic acceptance of the spectrometer, can then be removed from the beam by coarse collimation. Thus, the energy of essentially all  $\gamma$  rays reaching the nuclear target is known. This is very different from tagged-Bremsstrahlung beams which are always accompanied by very large numbers of untagged  $\gamma$  rays of unknown energy.

There are several advantages to tagging the backscattered  $\gamma$  ray beam: (1) The photon collimator can be large enough to accept most of the Compton scattering cross section. This results in a high total  $\gamma$ -ray flux. (2) Data from experiments may be accumulated over a large range of  $\gamma$  ray energies without changing the energy of the electron beam. Thus,  $\gamma$ -ray production does not require dedicated use of the ring. (3) The resolution attainable with tagging is significantly better than what can be achieved by collimation at these high energies. (4) The tagged  $\gamma$ -ray beam is much less sensitive to the tune of the storage ring, to small changes in electron beam phase space and position, and is almost completely insensitive to the electron divergence. Thus, there is now no necessity of pulsing the laser light and tagging results in a major simplification of the production method.

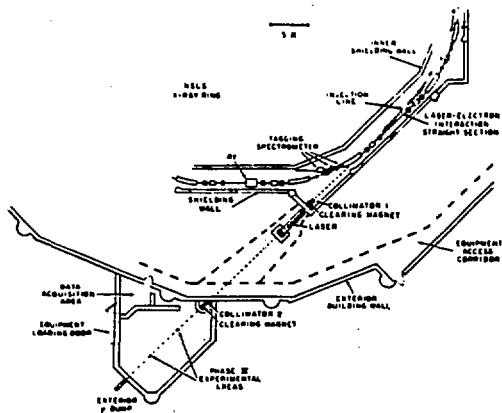


Fig. 4 A plan of the LEGS facility at BNL.

The planned layout of the laser-electron interaction region and the Y ray experimental areas is shown in Fig. 4. Initially, an Ar-Ion laser, operating external to the storage ring with 3 Watts in the UV (3511Å), will be used to produce  $10^7$  photons per second in the tagging interval from 175 MeV to 300 MeV. When the X-ray ring achieves 3.0 GeV, the Y-ray energy range will extend up to 420 MeV, and a higher powered laser will be used to double the flux.

The Tagging Spectrometer Coupled to the X-Ray Ring

The design of the spectrometer that will be used to momentum analyze the Compton scattered electrons has several unusual constraints, arising from its coupling with the storage ring. To preserve the ring symmetry, and hence the beam lifetime, no existing transport elements can be severly altered or moved. Furthermore, although at high energies the electron beam dimensions are tiny, a large transverse aperture is used when loading the ring at 0.7 GeV. Thus, the tagging spectrometer elements are confined to sit outside of the existing vacuum envelope. Finally, all spectrometer fringing fields must be effectively cancelled in the vicinity of the stored beam.

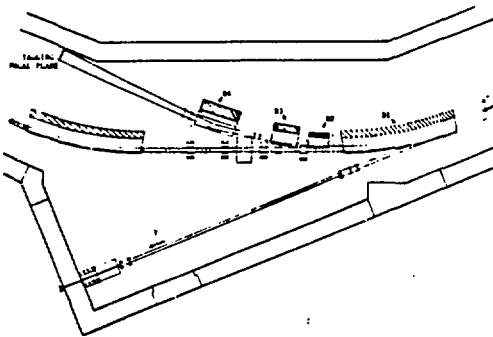


Fig. 5 The LEGS tagging spectrometer.

The LEGS spectrometer shown in Fig. 5 will consist of four dipole magnets (D1 through D4). The first magnet (D1) is the existing storage ring dipole,

located 5.5 m from the center of the electron-laser interaction region. The second dipole (D2) is a septum magnet, designed to sit just outside the existing ring vacuum chamber and accept the maximum dynamic energy range. The scattered electrons emerging from D2 then pass through an existing gap between the poles and the return yoke of a ring sextapole. The final two dipoles (D3 & D4) are of conventional construction.

The magnet D2 is of a somewhat unusual design, in that the current septum has been removed from the magnet gap and placed just outside the edge of the poles (Fig. 6). This has been done in order to reduce the width of the septum (by increasing its height) while maintaining an acceptable current density ( $4000 \text{ A/cm}^2$ ). The narrow width is essential to obtain a large dynamic range since the dispersion at D2, due to D1, is only  $0.30 \text{ mm/MeV}$ . This septum geometry results in an increased leakage field, but since the magnet is constrained by the existing vacuum envelope to be 8 gap lengths (5.5 cm) from the beam, the actual field at the position of the circulating beam is less than 40 gauss. This field will be cancelled by coils above and below the beam.

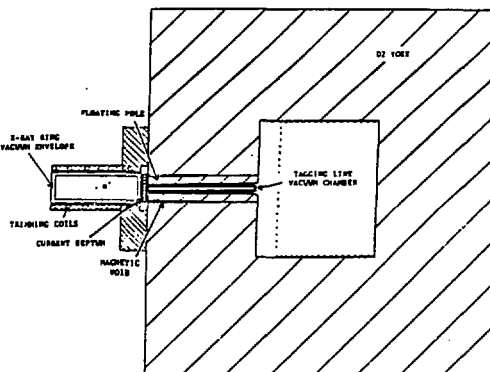


Fig. 6 Cross-sectional view of septum magnet D2.

To focus the Compton scattered electrons onto a focal plane, a quadrupole field is desirable before D3. Since there is no space for a separate element, a gradient (450 gauss/cm) will be introduced into D2, so that the field decreases from 1.1 kG at the septum to 9 kG at the inside. The increased fringing which would normally accompany such a design is reduced by using a floating pole tip.<sup>5)</sup>

Calculations with the code TRIM<sup>6)</sup> have been made to design the septum and trim coils for D2. The magnitude and shape of the leakage field at the stored beam can be adjusted by varying the height of the septum. The septum height (2.5 cm) is chosen to make the quadrupole field zero at the beam. Two sets of trim coils will be used to cancel higher multipoles. One set (COIL 1 in Fig. 7) has current symmetry chosen to cancel both dipole and sextupole components of the leakage field. A second coil (COIL 2 in Fig. 7) has only odd multipoles with geometry selected for no quadrupole field and current chosen to cancel the octupole component. The resulting fields calculated for the region near the beam are shown in Fig. 7. With both coils (1+2) the field is less than 0.5 gauss within 1 cm of the beam (0 in Fig. 7).

The first order optical properties of this tagging spectrometer have been computed with TRANSPORT.<sup>7)</sup> The energy resolution is better than 1.5 MeV which, when

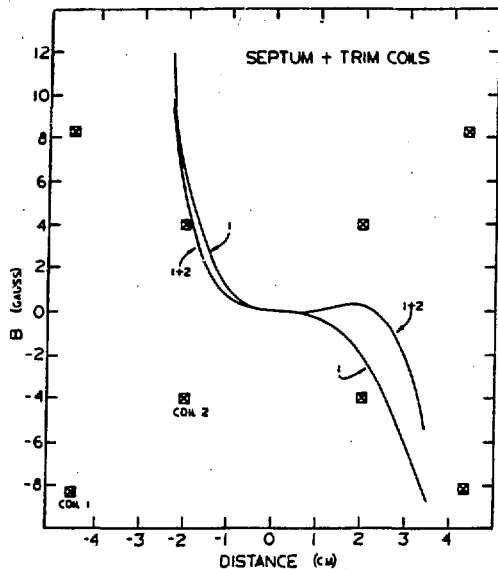


Fig. 7 Trimmed fields from D2 near the beam (at 0).

combined with the resolution of the ring,  $8 \times 10^{-4}$ , gives a total resolution of 2.3 MeV. Second order aberrations have been estimated and are negligible, principally because of the small divergence of the stored beam ( $< 0.1$  mrad).

#### Expected $\gamma$ -Ray Flux Levels

For an electron-laser interaction length  $L_L$ , an energy  $\epsilon_L$  per laser photon and a peak laser power  $P_L$  during the light pulse, and a stored electron current of  $I_e$ , the expected  $\gamma$ -ray flux is

$$Y_\gamma (\text{sec}^{-1}) = \frac{(2.60) I_e (\text{amps}) P_L (\text{Watts}) \sigma (\text{mb}) L_L (\text{cm})}{\epsilon_L (\text{eV}) A (\text{cm}^2)} \quad (3.1)$$

where  $\sigma$  is the laboratory cross section for backscattering, integrated over the  $\gamma$ -ray beam defining collimator, and  $A$  is the effective area of overlap of the laser and electron beams. If the electron beam has a Gaussian distribution in space characterized by half-widths  $\sigma_x$  and  $\sigma_y$ , and if the cylindrical laser beam has a Gaussian power distribution which falls off radially with half-width  $\sigma_L$ , then

$$A = 2\pi \sqrt{\sigma_L^2 + \sigma_x^2} \cdot \sqrt{\sigma_L^2 + \sigma_y^2} \quad (3.2)$$

The NSLS X-ray ring is designed for operation at  $I_e = 0.5$  amps with an extremely small beam size --  $\sigma_x = 0.4$  mm and  $\sigma_y = 0.07$  mm in the straight sections. This leads to a very high flux with only modest laser powers. For example, the Ar-Ion laser operating with 3 Watts in the UV ( $\sim 3511 \text{ \AA}$ ) is sufficient to produce over  $10^7$  tagged photons  $\text{s}^{-1}$ .

The number of  $\gamma$  rays backscattered through the beam-defining collimator (used to remove the low energy untagged component) depends not only upon the areas of the electron and laser beams, but also upon how these areas vary with position along the interaction region, and upon how the angular divergence of the electrons varies along the interaction length. These effects are

not included in Eq. (3). However, from Monte Carlo calculations we expect the resulting fluxes to be only a factor of 2 lower than would be predicted by Eq. (3).

There is a first order limitation on the flux of tagged  $\gamma$ -rays. If two  $\gamma$  rays, in the energy range defined by the coarse collimator and above the minimum acceptance of the tagging spectrometer (175 MeV), are produced within a single electron pulse, then two counters on the tagging focal plane will fire. Any resulting nuclear event must be discarded, unless the kinematics of the reaction can be used to determine which photon initiated the event. For the time structure of the pulses in the NSLS X-ray ring (1.5 ns bunches separated by 18.9 ns), this first order limit is  $2 \times 10^7 \text{ s}^{-1}$ . At this level the perturbation of the lifetime of the stored beam due to laser backscattering is small (15%).

The useful tagged flux can be increased further by retaining the events where two or more tagging counters fire. In most cases, the nuclear target would be thin enough so that only one of the associated  $\gamma$  rays would produce an event. This  $\gamma$  ray is in coincidence with its tagging electron but in random coincidence with others that reach the focal plane from the same electron bunch. The spectrum of these random events can be measured to a high accuracy and subtracted. The time structure of the NSLS beam differs from what is usually encountered with electron accelerators. In our case, the pulse pair resolution is irrelevant so long as events are processed on a bunch by bunch basis. The probability for a "Random" contribution to the spectrum is then governed by a Poisson rather than a Normal distribution. With this method, useful flux levels in excess of  $10^8 \text{ s}^{-1}$  are achievable with a Trues/Randoms ratio better than unity. However, these higher flux levels will lead to shorter ring lifetimes, and the extent to which this will be practical will depend on the filling time and the compatibility with other NSLS users.

#### Polarization

Because of the small spin-flip amplitude in backward Compton scattering, the  $\gamma$  ray beam retains most of the polarization of the incident laser light. The parallel component of the cross section is compared to the total (parallel + perpendicular) in Fig. 8, assuming a circular collimator and a linearly polarized laser beam. The ratio of these two, the polarization, is shown at the bottom of the figure. At all angles, and hence all  $\gamma$ -ray energies, the polarization is greater than about 75%. However, even this level can be greatly improved. The contamination of the beam with  $\gamma$  rays polarized perpendicular to the electric vector of the laser light  $\vec{P}_L$  comes from scattering into azimuthal angles near 0 or  $\pi$ , relative to  $\vec{P}_L$ . If a rectangular  $\gamma$ -ray collimator is used that is narrow in the direction of  $\vec{P}_L$ , the polarization of the transmitted flux can be dramatically increased. This is illustrated in Fig. 9. Here the results of Monte Carlo calculations are plotted for a circular (a) and a rectangular (b) collimator. (In (b),  $\sigma_x$  and  $\sigma_y$  are the half angles subtended by the collimator in planes perpendicular and parallel to  $\vec{P}_L$ , respectively.) The calculations include the effects of the variation of the electron beam size and angular divergence along the interaction region. The rectangular collimator reduces the transmitted flux by a factor of  $\sim 2.5$ , but increases the polarization to greater than 90%.

#### Extension to higher energies with a FEL

The 300 MeV (420 MeV) limit on the  $\gamma$ -ray energy arises from a lower limit of  $3500 \text{ \AA}$  on the wavelength of the laser light used for backscattering at 2.5 GeV

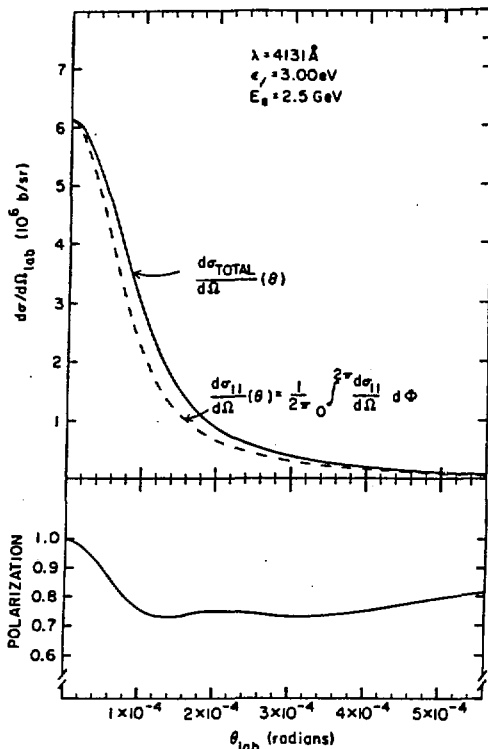


Fig. 8 Angular dependence of the  $\gamma$ -ray polarization.

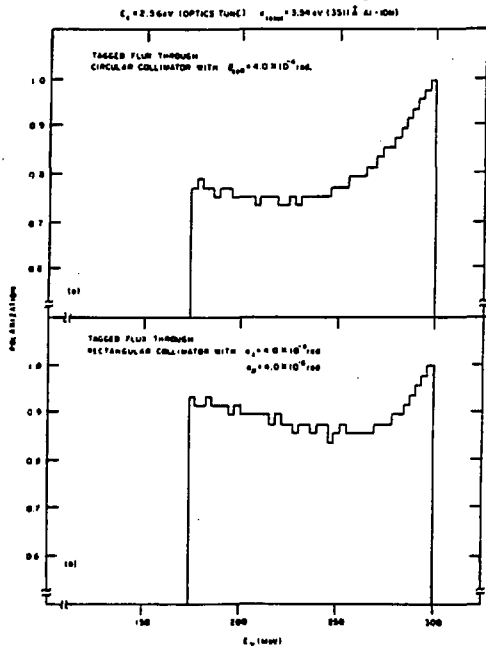


Fig. 9 Tagged- $\gamma$ -polarization for 2 collimator shapes.

(3 GeV). Lower wavelengths are commercially available by frequency-doubling lasers. However, such devices can operate with high duty-cycles only at power levels that are about  $10^3$  times smaller than the Ar-ion laser. The corresponding reductions in  $\gamma$ -ray flux would result in a beam of limited usefulness. An attractive way to increase the  $\gamma$ -ray energy, while maintaining a power level sufficient to produce a high flux, is to use a Free Electron Laser (FEL). This is a device in which photons and electrons together traverse a periodically varying magnetic field. The presence of photons and electrons inside this undulating field stimulates the emission of more photons of the same wavelength.

The wavelength of the photons emerging from an FEL is related to the periodicity  $\lambda_0$  of the magnetic field in the undulator and to the energy of the electron beam  $\gamma mc^2$  by

$$\lambda = \frac{\lambda_0}{2\gamma^2} (1 + K^2) \quad (4)$$

where the parameter  $K$  is proportional to the r.m.s. magnetic field. The construction of an FEL on a straight section of the  $E_s < 700$  MeV VUV ring at the NSLS is presently nearing completion, and it should be possible to obtain wavelengths as low as 2000  $\text{\AA}$  with electron energies of 300 to 600 MeV in this storage ring.

One might imagine such an FEL mounted on the X-ray ring with the resulting laser light arranged to backscatter from the 3 GeV electrons and produce ultra-high energy photons. However, the factor  $\gamma$  in Eq. (4) would then be 6000 and the required undulator and optical cavity are not realizable. The solution to this problem is unique to the NSLS at Brookhaven. Because of the proximity of the low-energy and high-energy storage rings, and because both rings can be run from the same Rf oscillator and thus synchronized in time, the light from the FEL on the VUV ring can be transported to the injection straight of the X-ray ring and there, backscattered. The power levels at 2000  $\text{\AA}$  expected from the VUV-FEL would produce a total tagged  $\gamma$ -ray flux of  $2 \times 10^7 \text{ sec}^{-1}$ , extending up to about 700 MeV. This coupling of the two NSLS storage rings is planned for the final phase of our project.

#### References

- 1) A.M. Sandoz, M.J. LeVine, C.E. Thorn, G. Giordano, and G. Matone, LEGS proposal, September 1982, BNL No. 32717; see also, Proc. Workshop on Use of Electron Rings for Nucl. Phys., Lund, Sweden, October 1982.
- 2) R.H. Milburn, Phys. Rev. Lett. **10**, 75 (1963); F.R. Arutyunian and V.A. Tumanian, Phys. Lett. **176** (1963).
- 3) J. Ballam, et al., Phys. Rev. Lett. **23**, 498 (1969).
- 4) G. Matone, et al., Lecture Notes in Phys. **62**, 149 (1977); L. Federici, et al., Il Nuovo Cim. **59B**, 247 (1980).
- 5) C.E. Thorn, et al., IEEE **NS-28**, 2089 (1981).
- 6) J.S. Colonias, Particle Accelerator Design: Computer Programs, Acad. Press, N.Y. (1974).
- 7) K.L. Brown and S.K. Howry, SLAC, No. 91 (1970).

## **DISCLAIMER**

This report was prepared as an account of work sponsored by an agency of the United States Government. Neither the United States Government nor any agency thereof, nor any of their employees, makes any warranty, express or implied, or assumes any legal liability or responsibility for the accuracy, completeness, or usefulness of any information, apparatus, product, or process disclosed, or represents that its use would not infringe privately owned rights. Reference herein to any specific commercial product, process, or service by trade name, trademark, manufacturer, or otherwise does not necessarily constitute or imply its endorsement, recommendation, or favoring by the United States Government or any agency thereof. The views and opinions of authors expressed herein do not necessarily state or reflect those of the United States Government or any agency thereof.